Published in final edited form as:

J Inherit Metab Dis. 2019 May ; 42(3): 459–469. doi:10.1002/jimd.12056.

Gene therapy prevents hepatic tumor initiation in murine glycogen storage disease type Ia at the tumor-developing stage

Jun-Ho Cho[1], **Young Mok Lee**[1,#], **Matthew F. Starost**[2], **Brian C. Mansfield**[1,3], and **Janice Y. Chou**[1,*]

[1]Section on Cellular Differentiation, Division of Translational Medicine, Eunice Kennedy Shriver National Institute of Child Health and Human Development, Bethesda, MD 20892, USA

[2]Division of Veterinary Resources, National Institutes of Health, Bethesda, MD 20892, USA

[3]Foundation Fighting Blindness, Columbia, MD 21046, USA

Abstract

Hepatocellular adenoma/carcinoma (HCA/HCC) is a long-term complication of glycogen storage disease type-Ia **(**GSD-Ia) which is caused by a deficiency in glucose-6-phosphatase-α (G6Pase-α or G6PC), a key enzyme in gluconeogenesis. Currently, there is no therapy to address HCA/HCC in GSD-Ia. We have previously shown that a recombinant adeno-associated virus (rAAV) vector-mediated *G6PC* gene transfer to 2-week-old *G6pc*−/− mice prevents HCA development. However, it remains unclear whether *G6PC* gene transfer at the tumor developing stage of GSD-Ia can prevent tumor initiation or abrogate the pre-existing tumors. Using liver-specific *G6pc*-knockout (L-*G6pc*−/−) mice that develop HCA/HCC, we now show that treating the mice at the tumor-developing stage with rAAV-G6PC restores hepatic G6Pase-α expression, normalizes glucose homeostasis, and prevents de novo HCA/HCC development. The rAAV-G6PC treatment also normalizes defective hepatic autophagy and corrects metabolic abnormalities in the non-tumor liver tissues of both tumor-free and tumor-bearing mice. However, gene therapy cannot restore G6Pase-α expression in the HCA/HCC lesions and fails to abrogate any pre-existing tumors. We show that the expression of 11 β-hydroxysteroid dehydrogenase type-1 that mediates local glucocorticoid activation is down-regulated in HCA/HCC lesions, leading to impairment in glucocorticoid signaling critical for gluconeogenesis activation. This suggests that local glucocorticoid action downregulation in the HCA/HCC lesions may suppress gene therapy mediated G6Pase-α restoration. Collectively, our data show that rAAV-mediated gene therapy can

*Correspondence should be addressed to: Janice Y. Chou, Building 10, Room 8N240C, NIH, 10 Center Drive, Bethesda, MD 20892-1830, Tel: 301-496-1094; Fax: 301-402-6035, chouja@mail.nih.gov.

#Current address: Glycogen Storage Disease Program, University of Connecticut School of Medicine, Farmington, Connecticut, USA

Details of the Contributions of Individual Authors:

Jun-Ho Cho designed and performed the research, analyzed data, and wrote the paper. Young Mok Lee performed the research and analyzed data. Matthew F. Starost performed pathological analysis. Brian C. Mansfield analyzed data and wrote the paper. Janice Y. Chou designed the research, analyzed data, and wrote the paper.

Conflict of Interest

Jun-Ho Cho, Young Mok Lee, Matthew F. Starost, Brian C. Mansfield, and Janice Y. Chou declare that they have no conflicts of interest.

Compliance with Ethics Guidelines

Animal Rights:

All institutional and national guidelines for the care and use of laboratory animals were followed.

prevent de novo HCA/HCC development in L-*G6pc*−/− mice at the tumor developing stage, but it cannot reduce any pre-existing tumor burden.

Keywords

Gene therapy; glucose-6-phosphatase-α; hepatocellular adenoma/carcinoma; autophagy; pre-receptor glucocorticoid signaling

Introduction

Glycogen storage disease type Ia (GSD-Ia, MIM232200) is caused by a deficiency in glucose-6-phosphatase-α (G6Pase-α or G6PC) that is expressed primarily in the liver, kidney, and intestine (Chou et al. 2010). G6Pase-α catalyzes the hydrolysis of glucose-6-phosphate (G6P) to glucose and phosphate in the terminal step of gluconeogenesis and glycogenolysis and is a key gluconeogenic enzyme for endogenous glucose production (Chou et al. 2010). GSD-Ia patients are unable to maintain glucose homeostasis and initially present with a life-threatening fasting hypoglycemia along with the long-term complication of hepatocellular adenoma (HCA) that develops in 75% of GSD-I patients over 25 years-old (Chou et al. 2010; Rake et al. 2002). In 10% cases, HCA undergoes malignant transformation to hepatocellular carcinoma (HCC) (Chou et al. 2010; Franco et al. 2005; Rake et al. 2002). Strict compliance to dietary therapies can address the life-threatening symptoms of GSD-I but does not prevent HCA/HCC risk. A recombinant adeno-associated virus (rAAV)-based gene augmentation therapy, that recently entered clinical trials (NCT03517085), has shown strong preclinical data for survival and metabolic normalization. We now further characterize the value of the gene therapy for pre-existing hepatic lesions in a preclinical mouse model.

We have generated G6Pase-α-deficient (*G6pc*−/−) mice that mimic the phenotype of human GSD-Ia (Lei et al. 1996). In past work, we have shown that 2-week-old *G6pc*−/− mice treated with rAAV-G6PC vector do not develop HCA over 70 weeks (Lee et al. 2012), suggesting that early restoration of hepatic G6Pase-α expression prevents tumor development. However, it remains unclear whether gene transfer at later stages of the GSD-Ia disorder can prevent tumor initiation or abrogate the pre-existing tumors. The *G6pc*−/− mice used in the proof of concept experiments are difficult to study because of the labor intense dietary therapy required for the mice to survive weaning (Lei et al. 1996). We therefore generated a liver-specific *G6pc*-deficient (L-*G6pc*−/−) mouse strain that survive to adulthood and develop HCA (Cho et al. 2017).

The major regulators of hepatic glucose metabolism are the glucocorticoids that promote gluconeogenesis and stimulate the expression of key gluconeogenic genes, *G6PC* and *PEPCK* (phosphoenolpyruvate carboxykinase) (Kuo et al. 2015; Patel et al. 2014). The local (pre-receptor) glucocorticoid activation is mediated by 11β-hydroxysteroid dehydrogenase type 1 (11βHSD1) that converts inert cortisone (in human) and dehydrocorticosterone (in rodents) into active cortisol and corticosterone, respectively (Czegle et al. 2012; Gathercole et al. 2013), allowing glucocorticoid receptor (GR) to be activated. Studies have shown that the expression of 11βHSD1 is down-regulated in HCC (Liu et al. 2016; Ma et al. 2013).

Furthermore, Wang et al. (2012) showed that the expression of *G6PC* and *PEPCK* was markedly decreased in HCC lesions, suggesting gluconeogenesis suppression.

In this study, we show that systemic rAAV-G6PC-mediated gene therapy of L-*G6pc*−/− mice prevents liver tumor initiation but fails to reduce tumor burden. Notably, G6Pase-α restoration was markedly suppressed in HCA/HCC lesions of the treated mice. We also show that in HCA/HCC lesions, 11βHSD1-mediated GR signaling is impaired, suggesting that down-regulation of local glucocorticoid action may suppress rAAV-G6PC-mediated G6Pase-α expression.

Materials and methods

Animals

All animal studies were conducted under an animal protocol approved by the Eunice Kennedy Shriver National Institute of Child Health and Human Development Animal Care and Use Committee. The liver-specific *G6pc*-deficient (L-*G6pc*−/−) and L-*G6pc*+/− mice were generated by tamoxifen-mediated excision of the *G6pc* exon 3 in 6-week-old $G6pc^{fx/fx}$.$SA^{creERT2/w}$ and $G6pc^{fx/w}$.$SA^{creERT2/w}$ mice, respectively, as previously described (Cho et al. 2017). GSD-Ia is an autosomal recessive disorder and the phenotypes of L-*G6pc* +/+ and L-*G6pc*+/− were indistinguishable, therefore both mice were used as controls. To reconstitute hepatic G6Pase-α activity, mice at 53 WP (weeks post *G6pc gene* deletion) were infused via retro-orbital sinus with rAAV-G6PC (Yiu et al. 2010) at 2×10^{12} viral particles (vp)/kg and analyzed at 78 WP. Liver samples were collected from mice following a 6-hour fast.

Quantitative real-time RT-PCR and Western blot analyses

The mRNA expression was quantified by real-time RT-PCR using the TaqMan probes (Life Technologies, Carlsbad, CA, USA) in an Applied Biosystems Quantstudio 3 Real-Time PCR System (Foster City, CA, USA). Data were normalized to 18S rRNA. Western blot images were detected with the use of the LI-COR Odyssey scanner and the Image studio 3.1 software (Li-Cor Biosciences, Lincoln, NE, USA). The antibodies used were β-actin (sc-47778) and PEPCK (sc-32879) from Santa Cruz Biotechnology (Dallas, TX, USA); LC3B (ab51520) and Laminin Receptor (ab133645) from Abcam (Cambridge, MA, USA); p62 (NBP1–49956) from Novus Biologicals (Littleton, CO, USA); ATG3 (#3415) and GR (#12041) from Cell Signaling Technology (Danvers, MA, USA); SIRT1 (#07–131) antibody was purchased from Millipore; 11βHSD1 (#10004303) from Cayman chemical (Ann Arbor, MI, USA). The monoclonal antibody against human G6Pase-α has been previously described (Cho et al. 2017).

Metabolites determinations

Liver lysates were deproteinized using 14% (wt/vol) perchloric acid, and then neutralized with 2 M KOH/0.2 M MOPS. The levels of glucose and G6P in deproteinized lysates were determined using the respective assay kit from BioVision (Mountain View, CA, USA). Hepatic levels of glycogen and triglyceride were determined using a Glycogen and a

Triglyceride Quantification Kit (Biovision), respectively. Microsome isolation and G6Pase-α activity assay were performed as described (Yiu et al. 2010).

Enzyme histochemical analysis of G6Pase-α activity

Enzyme histochemical analysis of G6Pase-α activity was performed as described previously (Yiu et al. 2010). Briefly, 10-μm thick liver cryosections were for 10 minutes at room temperature in a solution containing 40 mM Tris-maleate pH 6.5, 10 mM glucose-6-phosphate, 300 mM sucrose, and 3.6 mM lead nitrate. The trapped lead phosphate generated by G6Pase-α activity was visualized following conversion to the brown colored lead sulfide.

Immunohistochemical analysis

Mouse liver tissues were fixed in 10% neutral buffered formalin (Fisher Scientific, Grand Island, NY, USA), embedded in paraffin, then sectioned to 10 μm thickness, and the paraffin was removed by Xylene (Fisher Scientific). Liver sections were then incubated in antigen unmasking solution (Vector Laboratories, Burlingame, CA, USA) for 10 min at 100°C. Endogenous peroxidases were quenched with 0.9% hydrogen peroxide in methanol, and then blocked with the Avidin/Biotin Blocking Kit (Vector Laboratories). The sections were then incubated with the antibody against anti-GR (Cell Signaling) and followed with the appropriate biotinylated secondary antibodies (Vector Laboratories). The resulting complexes were detected with an ABC kit using the DAB Substrate (Vector Laboratories). Sections were also counterstained with hematoxylin (Sigma-Aldrich, St. Louis, MO, USA) and visualized using a Zeiss Axioskop2 plus microscope equipped with 10X/0.45NA, 20X/0.5NA or 40X/0.75NA objectives (Carl Zeiss, Oberkochen, Germany).

Magnetic resonance imaging

Tumors in mice were monitored by MRI using a 7T Bruker Biospec (Bruker-Biospin, Ettlingen, Germany) at the NIH mouse imaging facility following the standard procedures. Briefly, mice were anesthetized using 5% isoflurane (Abbott Laboratories, North Chicago, IL), transferred to a cradle that maintains anesthetization, and then into the MRI scanner. The liver and abdomen images were acquired using a rapid acquisition with relaxation enhancement sequence (Bruker-Biospin). The imaging parameters were $TR/TE_{Effective}$ = 2000/20.6 ms, Number of Echoes = 4, slice thickness = 1 mm, field of view = 3 cm, number of averages = 8, and imaging matrix = 256 × 256. Acquisition was gated to the breathing signal to reduce motion artifacts.

Vector copy number analysis

Total DNA was isolated from liver, tumor, and kidney tissues using the DNeasy Blood & Tissue Kit (Qiagen). The vector genome copy numbers were quantified by real-time RT-PCR in an Applied Biosystems Quantstudio 3 Real-Time PCR System using TagMan probes: human *G6PC* gene, Hs00609178_m1. Plasmid DNA corresponding to 0.01 to 100 copies of h*G6PC* gene was used in a standard curve. The vector genome copy numbers per 1 ng of genomic DNA were obtained by comparing the Ct values of samples to the standard curve.

Statistical analysis

The unpaired *t* test was performed by using the GraphPad Prism Program, version 4 (San Diego, CA). The values were considered statistically significant at $P < 0.05$.

Results

Metabolic alterations and autophagy impairment persisted in the livers of L-*G6pc*−/− mice

We have generated L-*G6pc*−/− mice to study long-term hepatic complications in GSD-Ia (Cho et al. 2017). Histopathological analysis showed that none of the L-*G6pc*−/− mice developed tumors at the pre-tumor stage of 12 WP (weeks post *G6pc gene* deletion) and 24 WP. Magnetic resonance imaging (MRI) analysis showed that 30% of L-*G6pc*−/− mice developed tumors at 53 WP (Fig. 1a) and histopathological analysis showed that 100% mice developed HCA/HCC at 78 WP (Fig. 1b). Pathological analysis revealed that tumor nodules less than 8.5 mm in diameter were mostly HCAs, characterized by a lack of portal tracts and compressed adjacent parenchyma, and nodules larger than 10 mm in diameter were mostly HCCs, consisting of anisocytotic and anisokaryotic hepatocytes (Fig. 1c).

Using L-*G6pc*−/− mice, we examined metabolic alterations associated with GSD-Ia at the pre-tumor (12 WP and 24 WP) and the tumor-developing (53 WP) stages. L-*G6pc*−/− mice displayed hepatomegaly, reduced hepatic glucose levels, and increased hepatic levels of G6P, glycogen, triglyceride at both pre-tumor and tumor-developing stages (Fig. 2a). Using L-*G6pc*−/− mice at 12 WP, we have previously shown that hepatic G6Pase-α deficiency-mediated autophagy impairment is mediated by down-regulation of sirtuin 1 (SIRT1) signaling (Cho et al. 2017). We now show that hepatic SIRT1 expression remained suppressed in L-*G6pc*−/− mice at the tumor-developing stages (Fig. 2b). Consistently, the expression of phosphatidylethanolamine-conjugated microtubule-associated protein 1 light chain 3B-II (LC3B-II), a marker of autophagosome formation were decreased at both stages (Fig. 2b), suggesting sustained autophagy impairment. Studies have shown that the autophagy impairment leads to accumulation of p62, an autophagy specific substrate that promotes tumorigenesis (Inami et al. 2011; Takamura et al. 2011). Indeed, compared to control mice, hepatic levels of p62 were markedly higher in L-*G6pc*−/− mice at both pre-tumor and tumor-developing stages (Fig. 2b). Collectively, hepatic G6Pase-α deficiency leads to persistent metabolic alterations and autophagy impairment.

rAAV-mediated gene transfer to L-*G6pc*−/− mice at the tumor-developing stage prevents tumor initiation but cannot reduce tumor burden

We have shown that rAAV-G6PC-mediated restoration of hepatic G6Pase-α expression in L-*G6pc*−/− mice at 12 WP normalizes metabolic abnormalities and autophagy impairment, both of which can contribute to hepatic tumorigenesis in GSD-Ia (Cho et al. 2017, 2018). Therefore, we examined whether rAAV-mediated hepatic G6Pase-α restoration would prevent HCA/HCC formation in L-*G6pc*−/− mice at the tumor-developing stage of 53 WP. MRI analysis of L-*G6pc*−/− mice at 53 WP had identified 8 tumor-free and 3 tumor-bearing (mouse-1, mouse-2, and mouse-3) mice. The tumor-bearing mouse-1 harbored 3 nodules, mouse-2 harbored 2 large tumor spots, each of which contained several super-imposed tumor nodules that could not be accurately accessed by MRI, and mouse-3 harbored 4

nodules. At 53 WP, we treated all 11 mice with rAAV-G6PC using untreated and age-matched L-*G6pc*−/− mice (n = 12) as controls. As expected at 78 WP, all untreated L-*G6pc*−/− mice developed HCA/HCC. At 78 WP, the 8 rAAV-treated mice with no pre-existing tumor remained HCA-free, while the 3 mice with pre-existing tumors remained HCA/HCC-bearing. Histopathological analysis showed that mouse-1 and mouse-3 harbored 3 and 4 nodules, respectively, and to our best estimation, mouse-2 harbored at least 5 overlapping tumor nodules. Importantly, the numbers of tumor nodules in mouse-1 and mouse-3 remained the same both by MRI analysis at 53 WP and by histopathological analysis at 78 WP. Collectively, these data indicate that rAAV-G6PC-mediated gene therapy can prevent tumor initiation but cannot reduce tumor burden.

We then examined G6Pase-α activity in both nontumor liver tissues and the tumor nodules at 78 WP. In the nontumor liver tissues, G6Pase-α activity was restored to 53% and 31% of normal hepatic G6Pase-α activity in tumor-free and tumor-bearing mice, respectively (Fig. 3a). Notably, in rAAV-G6PC treated tumor-bearing mice, G6Pase-α activity of the HCA/HCC lesions was 6% of wild-type activity, significantly lower than that of the adjacent non-tumor liver tissues. Supporting this, human *G6PC* mRNA expression mediated by rAAV-G6PC was significantly lower in the HCA/HCC lesions, compared to the adjacent non-tumor tissues (Fig. 3b). Enzyme histochemical analysis showed that G6Pase-α in wild type mice was distributed throughout the liver with significantly higher levels in proximity to blood vessels, and there was no stainable G6Pase-α activity in the liver sections of untreated L-*G6pc*−/− mice (Fig. 3c). In rAAV-treated L-*G6pc*−/− mice at 78 WP, G6Pase-α was distributed throughout in the non-tumor regions of the liver section with foci containing markedly higher levels of enzymatic activity (Fig. 3c). In contrast, there was little or no stainable G6Pase-α activity in the tumor lesions (Fig. 3c).

Phenotype analysis at 78 WP showed that the nontumor liver sections of all rAAV-treated L-*G6pc*−/− mice exhibited no histological abnormalities (Fig. 3d). Restoration of hepatic G6Pase-α expression also normalized liver weight in the 8 tumor-free mice, although the rAAV-treated tumor-bearing mice continued manifesting hepatomegaly (Fig. 3e). Compared to the control mice at 53 WP, the tumor-free L-*G6pc*−/− mice exhibited lower fasting blood glucose levels which were further reduced in the tumor-bearing mice (Fig. 3f). At 78 WP, fasting glucose tolerance profiles of wild-type and all rAAV-treated L-*G6pc*−/− mice were indistinguishable (Fig. 3f).

rAAV-mediated gene transfer to L-*G6pc*−/− mice at the tumor-developing stage normalizes defective hepatic autophagy and corrects metabolic abnormalities

Western-blot analysis confirmed that all L-*G6pc*−/− mice treated with rAAV-G6PC at 53 WP expressed significant high levels of G6Pase-α at 78 WP (Fig. 4a). Hepatic G6Pase-α restoration also increased levels of LC3B-II, ATG3 and reduced levels of p62 in tumor-free and tumor-bearing mice, indicating normalization of defective autophagy. One exceptional increase of p62 in the non-tumor liver tissue of mouse-2 (Fig. 4a, lane 11) which harbored multiple small nodules might be caused by contamination of tumor nodules. rAAV-G6PC-mediated gene transfer at 53 WP also corrected hepatic metabolic abnormalities in both groups of L-*G6pc*−/− mice. At 78 WP, hepatic glucose levels were markedly increased,

along with reduced hepatic levels of G6P, lactate, and triglyceride, although glycogen storage remained significantly elevated (Fig. 4b). Oil red O staining confirmed that rAAV-G6PC treatment normalized hepatic steatosis both in tumor-free and tumor-bearing mice (Fig. 4c).

Down-regulation of pre-receptor glucocorticoid action in the tumor lesions of rAAV-treated L-*G6pc*−/− mice

We have shown that rAAV-G6PC-mediated gene transfer restored high levels of G6Pase-α expression in the non-tumor liver tissues of the tumor-bearing L-*G6pc*−/− mice but only low levels of G6Pase-α were detectable in their HCA/HCC lesions (Fig. 3a-c). This suggests that either tumors are not transduced efficiently by the rAAV vector or that G6Pase-α expression is down-regulated in the malignantly transformed cells. We showed that the expression of cellular receptor for AAV8, the laminin receptor (LamR) (Akache et al. 2006) is similar between non-tumor tissues and HCA/HCC lesions (Fig. 5a), suggesting resistance to viral transduction may not have been a limiting factor.

We then examined vector genome copy numbers in the livers and tumors of rAAV-treated L-G6pc−/− mice as well as in their kidneys. The results showed that vector genome copy numbers in the non-tumor liver tissues were statistically indistinguishable between rAAV-treated tumor-free and tumor-bearing mice (Fig. 5b), suggesting that the transduction efficiency of rAAV is similar between the two groups of mice. However, compared to the non-tumor liver tissues, vector genome copy numbers in HCA/HCC lesions of the rAAV-treated mice were significantly lower (Fig. 5b). The apparent decrease in vector genome copy number values in tumor lesions could be caused by the fast rate of tumor cell proliferation. Studies have shown that kidney could not be effectively transduced by AAV8 (Lee et al 2013). As expected, extremely low but similar values of vector genome copy number were found in the kidney tissues of rAAV-treated tumor-free and tumor-bearing mice (Fig. 5b).

The glucocorticoid action is mediated by binding of the active glucocorticoids to the GR, nuclear translocation of the ligand-receptor-complex, and activation of the target genes (Kuo et al. 2015; Patel et al. 2014). In the rAAV-G6PC vector (Yiu et al. 2010), the *G6PC* promoter/enhancer that direct *G6PC* expression includes nucleotides −2864 to −1 of human *G6PC* 5' flanking sequences that contains several glucocorticoid response elements (Hutton & O'Brien, 2009; Vander Kooi et al, 2005). The local (pre-receptor) glucocorticoid activation is mediated by 11βHSD1 (Czegle et al. 2012; Gathercole et al. 2013). Intriguingly, during tumor development of the L-*G6pc*−/− mice, protein levels of 11βHSD1 decrease, with levels of 11βHSD1 highest in non-tumor regions of HCA-bearing mice, followed by HCA nodules, non-tumor regions of HCC-bearing mice, and HCC nodules (Fig. 5a). The *GR* mRNA levels were similar between the non-tumor liver tissues and the HCA/HCC lesions (Fig. 5c). Consistent with the attenuated expression of 11βHSD1 in the tumor lesions, nuclear translocation of GR was markedly reduced (Fig. 5d), suggesting suppressed glucocorticoid signaling. Supporting this, mRNA (Fig. 5e) and protein (Fig. 5f) levels of PEPCK, another gluconeogenic gene targeted by the GR, was also decreased in the HCA/HCC lesions of the L-*G6pc*−/− mice. Collectively, these results suggest that down-

regulation of glucocorticoid signaling may result in the markedly reduced G6Pase-α expression in the HCA/HCC lesions of rAAV-treated L-*G6pc*−/− mice.

Discussion

GSD-Ia is a juvenile lethal disease lacking a curative therapy (Chou et al. 2010). Dietary therapies have enabled GSD-Ia patients to attain near normal growth and pubertal development, but chronic complications including HCA/HCC remain (Chou et al. 2010; Rake et al. 2002). In long-term, over 70-week studies, we have shown that the *G6pc*−/− mice receiving rAAV-G6PC-mediated gene transfer at 14 days of age maintain glucose homeostasis and do not develop HCA (Lee et al. 2012). However, the efficacy of gene therapy in tumor initiation and abrogation in GSD-Ia animal model at the tumor-developing stage remains unknown. Using tumor-free and tumor-bearing L-*G6pc*−/− mice at tumor-developing stage of 53 WP, we show that rAAV-G6PC delivered the G6Pase-α transgene to the non-tumor liver sections of the mice and prevented HCA/HCC initiation. However, rAAV-G6PC-mediated gene transfer failed to restore G6Pase-α expression in the tumor lesions and the pre-existing tumors remained, indicating that early intervention, prior to the development of HCA/HCC, offers the best long-term outcomes. Finally, we show that the 11βHSD1-mediated local glucocorticoid action is downregulated in the HCA/HCC lesions, which may suppress G6Pase expression and prevent tumor abrogation.

Using L-*G6pc*−/− mice at the tumor-developing stage of 53 WP, we showed that rAAV-G6PC-mediated gene transfer efficiently restored G6Pase-α expression in the non-tumor liver tissues of the treated mice but failed to restore significant levels of G6Pase-α expression in the tumor lesions. The available evidence suggests that downregulation of glucocorticoid signaling in the tumor lesions of rAAV-treated L-*G6pc*−/− mice might suppress restoration of G6Pase-α expression and tumor abrogation. The transduction efficiency of the tumors to AAV8 appeared to be intact because the expression of the LamR, a cellular receptor for AAV8 (Akache et al. 2006) was similar between non-tumor tissues and HCA/HCC lesions. However, the expression of 11β-HSD1 that regulates the availability of active glucocorticoid at the pre-receptor level was decreased in the tumor lesions, leading to downregulation of glucocorticoid signaling and inhibition of gluconeogenesis. Accordingly, in the HCA/HCC lesions, the rAAV-mediated G6Pase-α restoration was suppressed along with reduced expression of *Pepck*, another key gluconeogenic gene. Ma et al. (2013) have recently shown that administration of dexamethasone, a synthetic glucocorticoid to a murine xenograft model of HCC resulted in stimulation of PEPCK and G6Pase-α expression and reduction in tumor growth. This suggests that a combinational therapy consisting of rAAV-G6PC-mediated gene transfer and strategies that could increase 11βHSD1 expression and stimulate local glucocorticoid signaling may be a worthy avenue to reduce or abrogate tumor lesions in GSD-Ia at the tumor-bearing stage.

Studies have shown that HCA formation in GSD-I is impacted by metabolic controls (Wang et al. 2011; Beegle et al. 2015; Dambska et al. 2017). Wang et al. (2011) showed that a lower rate of HCA formation correlated with good metabolic controls that reduce triglyceride concentrations in GSD-Ia patients. Subsequently, Beegle et al. (2015) showed that improved metabolic control in GSD-Ia patients could lead to the regression of pre-existing HCA. In

this study, we showed that rAAV-G6PC-mediated gene transfer normalized hepatic triglyceride levels and prevented tumor initiation in both tumor-free and tumor-bearing L-*G6pc*−/− mice, although it failed to reduce pre-existent tumor burden. However, we do not know whether gene therapy can affect the progression/regression of HCA. Unlike human GSD-Ia patients and the global *G6pc*−/− mice, L-*G6pc*−/− mice with normal kidney and intestine function can maintain blood glucose level to survive in the absence of any therapies (Cho et al. 2017). We have shown that that rAAV-treated *G6pc*−/− mice expressing ≥3% of normal hepatic G6Pase-α activity but lacking G6Pase-α restoration in the kidney and intestine, maintain glucose homeostasis, do not develop HCA and display physiologic features mimicking animals living under calorie restriction (Kim et al. 2015). It is possible that GSD-Ia patients receiving a liver-directed gene transfer will display physiologic features of calorie restriction which may play a beneficial role in abrogating or reducing the tumor burden after gene transfer.

In summary, we show that rAAV-G6PC-mediated gene therapy, which is now in phase I/II clinical trial for human GSD-Ia (NCT03517085), restores hepatic G6Pase-α expression, normalizes defective hepatic autophagy, prevents tumor initiation but cannot abrogate the established tumors. In the HCA/HCC lesions of the rAAV-G6PC-treated mice, down-regulation of 11βHSD1-mediated local glucocorticoid activation may suppress G6Pase-α restoration and prevent tumor abrogation.

Acknowledgements

We thank Dr. Pierre Chambon for the gift of the AlbCreERT2 mice, Dr. Martin Lizak for magnetic resonance imaging acquisitions, and Dr. Woo Kyun Bae for reading of magnetic resonance images.

Funding

This work was supported by the Intramural Research Program of the Eunice Kennedy Shriver National Institute of Child Health and Human Development, National Institutes of Health; and by the Children's Fund for Glycogen Storage Disease Research.

Abbreviations

GSD-Ia	glycogen storage disease type Ia
G6Pase-α or G6PC	glucose-6-phosphatase-α
HCA	hepatocellular adenoma
HCC	hepatocellular carcinoma
L-*G6pc*−/−	liver-specific G6pc-knockout, 11βHSD1, 11 β-hydroxysteroid dehydrogenase type-1
G6P	glucose-6-phosphate
rAAV	recombinant adeno-associated virus
WP	weeks post G6pc gene deletion
PEPCK	phosphoenolpyruvate carboxykinase

GR	glucocorticoid receptor
MRI	Magnetic resonance imaging
SIRT1	sirtuin 1
LC3	microtubule-associated protein 1 light chain 3
LamR	laminin receptor

References

Akache B, Grimm D, Pandey K, Yant SR, Xu H, Kay MA (2006) The 37/67-kilodalton laminin receptor is a receptor for adeno-associated virus serotypes 8, 2, 3, and 9. J Virol 80: 9831–9836 [PubMed: 16973587]

Beegle RD, Brown LM, Weinstein DA (2015) Regression of hepatocellular adenomas with strict dietary therapy in patients with glycogen storage disease type I. JIMD Rep 18: 23–32 [PubMed: 25308557]

Cho JH, Kim GY, Mansfield BC, Chou JY (2018) Hepatic glucose-6-phosphatase-alpha deficiency leads to metabolic reprogramming in glycogen storage disease type Ia. Biochem Biophys Res Commun 498: 925–931 [PubMed: 29545180]

Cho JH, Kim GY, Pan CJ et al. (2017) Downregulation of SIRT1 signaling underlies hepatic autophagy impairment in glycogen storage disease type Ia. PLoS Genet 13: e1006819 [PubMed: 28558013]

Chou JY, Jun HS, Mansfield BC (2010) Glycogen storage disease type I and G6Pase-beta deficiency: etiology and therapy. Nat Rev Endocrinol 6: 676–688 [PubMed: 20975743]

Czegle I, Csala M, Mandl J, Benedetti A, Karadi I, Banhegyi G (2012) G6PT-H6PDH-11betaHSD1 triad in the liver and its implication in the pathomechanism of the metabolic syndrome. World J Hepatol 4: 129–138 [PubMed: 22567185]

Dambska M, Labrador EB, Kuo CL, Weinstein DA (2017) Prevention of complications in glycogen storage disease type Ia with optimization of metabolic control. Pediatr Diabetes 18: 327–331 [PubMed: 28568353]

Franco LM, Krishnamurthy V, Bali D et al. (2005) Hepatocellular carcinoma in glycogen storage disease type Ia: a case series. J Inherit Metab Dis 28: 153–162 [PubMed: 15877204]

Gathercole LL, Lavery GG, Morgan SA et al. (2013) 11beta-Hydroxysteroid dehydrogenase 1: translational and therapeutic aspects. Endocr Rev 34: 525–555 [PubMed: 23612224]

Hutton JC, O'Brien RM (2009) Glucose-6-phosphatase catalytic subunit gene family. J Biol Chem 284: 29241–29245 [PubMed: 19700406]

Inami Y, Waguri S, Sakamoto A et al. (2011) Persistent activation of Nrf2 through p62 in hepatocellular carcinoma cells. J Cell Biol 193: 275–284 [PubMed: 21482715]

Kim GY, Lee YM, Cho JH et al. (2015) Mice expressing reduced levels of hepatic glucose-6-phosphatase-alpha activity do not develop age-related insulin resistance or obesity. Hum Mol Genet 24: 5115–5125 [PubMed: 26089201]

Kuo T, McQueen A, Chen TC, Wang JC (2015) Regulation of Glucose Homeostasis by Glucocorticoids. Adv Exp Med Biol 872: 99–126 [PubMed: 26215992]

Lee YM, Jun HS, Pan CJ et al. (2012) Prevention of hepatocellular adenoma and correction of metabolic abnormalities in murine glycogen storage disease type Ia by gene therapy. Hepatology 56: 1719–1729 [PubMed: 22422504]

Lee YM, Pan CJ, Koeberl DD, Mansfield BC, Chou JY (2013) The upstream enhancer elements of the G6PC promoter are critical for optimal G6PC expression in murine glycogen storage disease type Ia. Mol Genet Metab 110: 275–280 [PubMed: 23856420]

Lei KJ, Chen H, Pan CJ et al. (1996) Glucose-6-phosphatase dependent substrate transport in the glycogen storage disease type-1a mouse. Nat Genet 13: 203–209 [PubMed: 8640227]

Liu X, Tan XL, Xia M et al. (2016) Loss of 11betaHSD1 enhances glycolysis, facilitates intrahepatic metastasis, and indicates poor prognosis in hepatocellular carcinoma. Oncotarget 7: 2038–2053 [PubMed: 26700460]

Ma R, Zhang W, Tang K et al. (2013) Switch of glycolysis to gluconeogenesis by dexamethasone for treatment of hepatocarcinoma. Nat Commun 4: 2508 [PubMed: 24149070]

Patel R, Williams-Dautovich J, Cummins CL (2014) Minireview: new molecular mediators of glucocorticoid receptor activity in metabolic tissues. Mol Endocrinol 28: 999–1011 [PubMed: 24766141]

Rake JP, Visser G, Labrune P, Leonard JV, Ullrich K, Smit GP (2002) Glycogen storage disease type I: diagnosis, management, clinical course and outcome. Results of the European Study on Glycogen Storage Disease Type I (ESGSD I). Eur J Pediatr 161 Suppl 1: S20–S34 [PubMed: 12373567]

Takamura A, Komatsu M, Hara T et al. (2011) Autophagy-deficient mice develop multiple liver tumors. Genes Dev 25: 795–800 [PubMed: 21498569]

Vander Kooi BT, Onuma H, Oeser JK et al. (2005) The glucose-6-phosphatase catalytic subunit gene promoter contains both positive and negative glucocorticoid response elements. Mol Endocrinol 19: 3001–3022 [PubMed: 16037130]

Wang B, Hsu SH, Frankel W, Ghoshal K, Jacob ST (2012) Stat3-mediated activation of microRNA-23a suppresses gluconeogenesis in hepatocellular carcinoma by down-regulating glucose-6-phosphatase and peroxisome proliferator-activated receptor gamma, coactivator 1 alpha. Hepatology 56: 186–197 [PubMed: 22318941]

Wang DQ, Fiske LM, Carreras CT, Weinstein DA (2011) Natural history of hepatocellular adenoma formation in glycogen storage disease type I. J Pediatr 159: 442–446 [PubMed: 21481415]

Yiu WH, Lee YM, Peng WT et al. (2010) Complete normalization of hepatic G6PC deficiency in murine glycogen storage disease type Ia using gene therapy. Mol Ther 18: 1076–1084 [PubMed: 20389290]

Synopsis:

rAAV-G6PC-mediated gene transfer can prevent tumor initiation in murine GSD-Ia at the tumor developing stage, but it cannot reduce pre-existing tumor burden. Downregulation of local glucocorticoid action in the HCA/HCC lesions may suppress G6Pase-α restoration and prevent tumor abrogation.

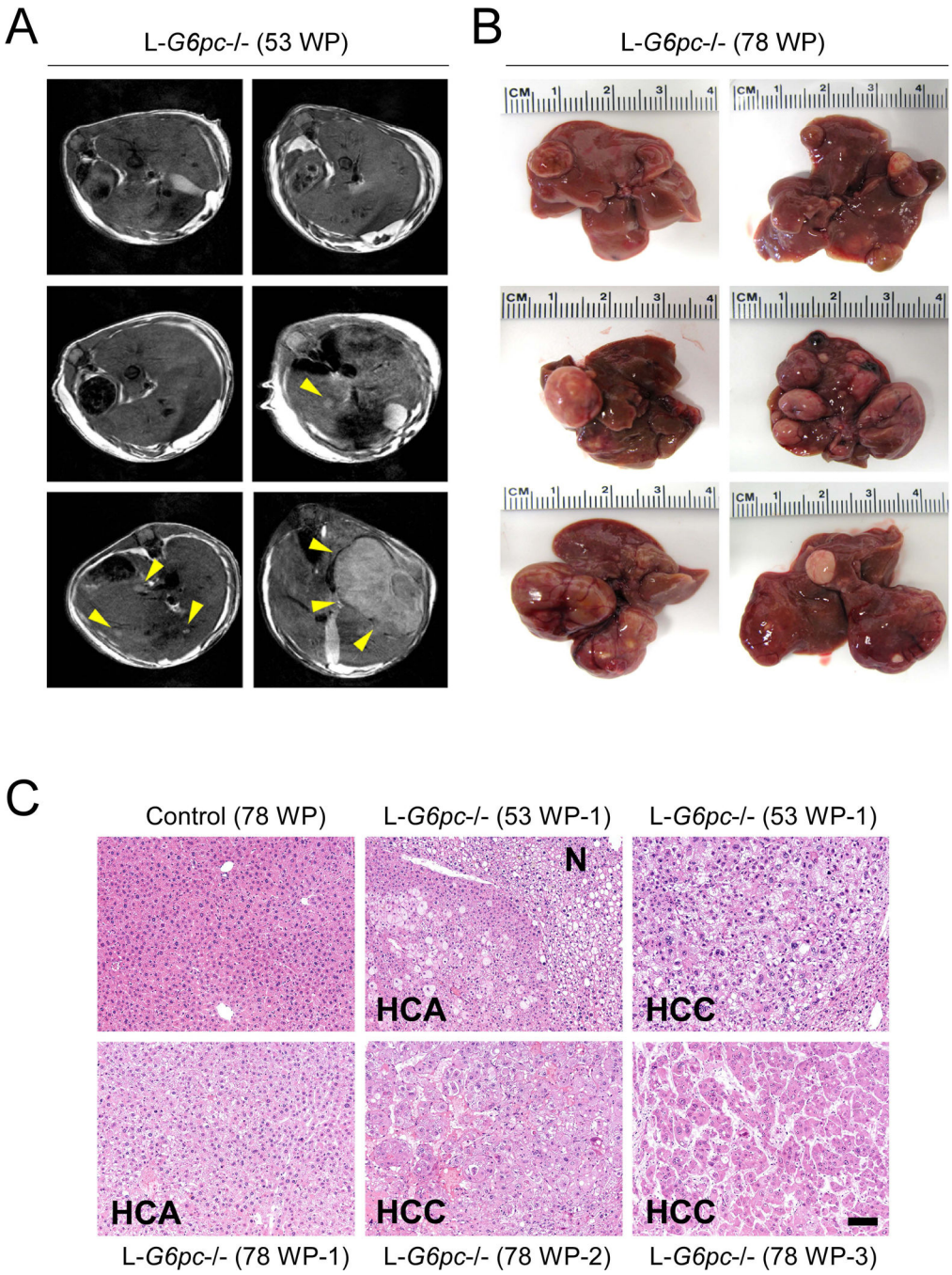

Fig. 1.

L-*G6pc*−/− mice develop HCA or HCC lesions. (**a**) Representative T2-weighted axial magnetic resonance image of L-*G6pc*−/− mice at 53 WP (weeks post *G6pc* gene deletion). Arrowheads indicate tumors. (**b**) Representative liver images of L-*G6pc*−/− mice at 78 WP. (**c**) Hematoxylin and eosin (H&E) stained liver sections. Scale bar, 100 μm. N denotes nontumor region of L-*G6pc*−/− mice.

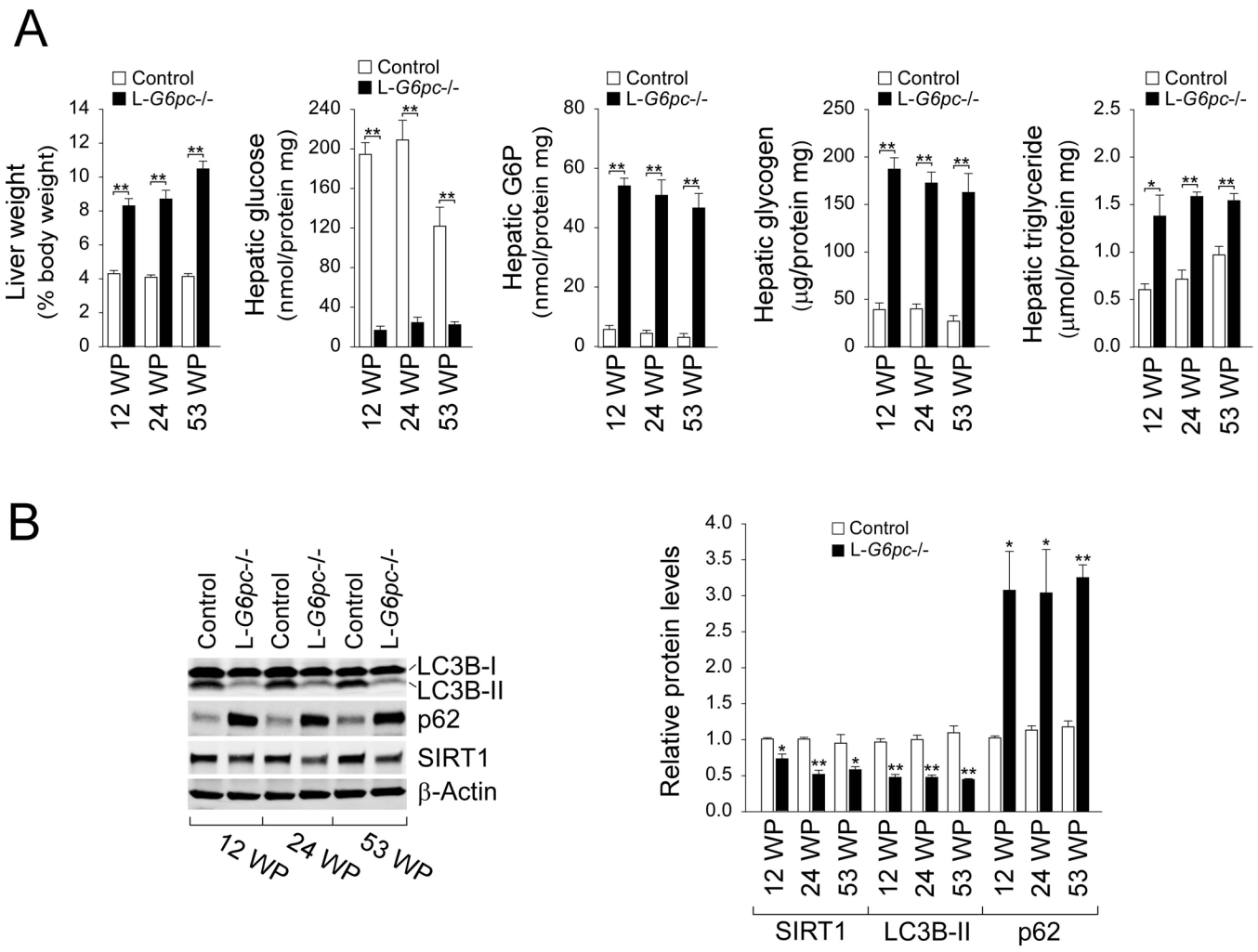

Fig. 2.

The livers of L-*G6pc*−/− mice exhibit persistent autophagy impairments and metabolic abnormalities. (**a**) Liver weights of control (n = 10) and L-*G6pc*−/− (n = 8–10). The levels of hepatic metabolites in control (n = 4) and L-*G6pc*−/− (n = 4) mice at 12, 24 and 53 WP. (**b**) Western blot analysis of the indicated hepatic proteins in control and L-*G6pc*−/− mice at 12, 24 and 53 WP, and quantification by densitometry (n = 3). Data represent the mean ± SEM. **P* < 0.05, ***P* < 0.005.

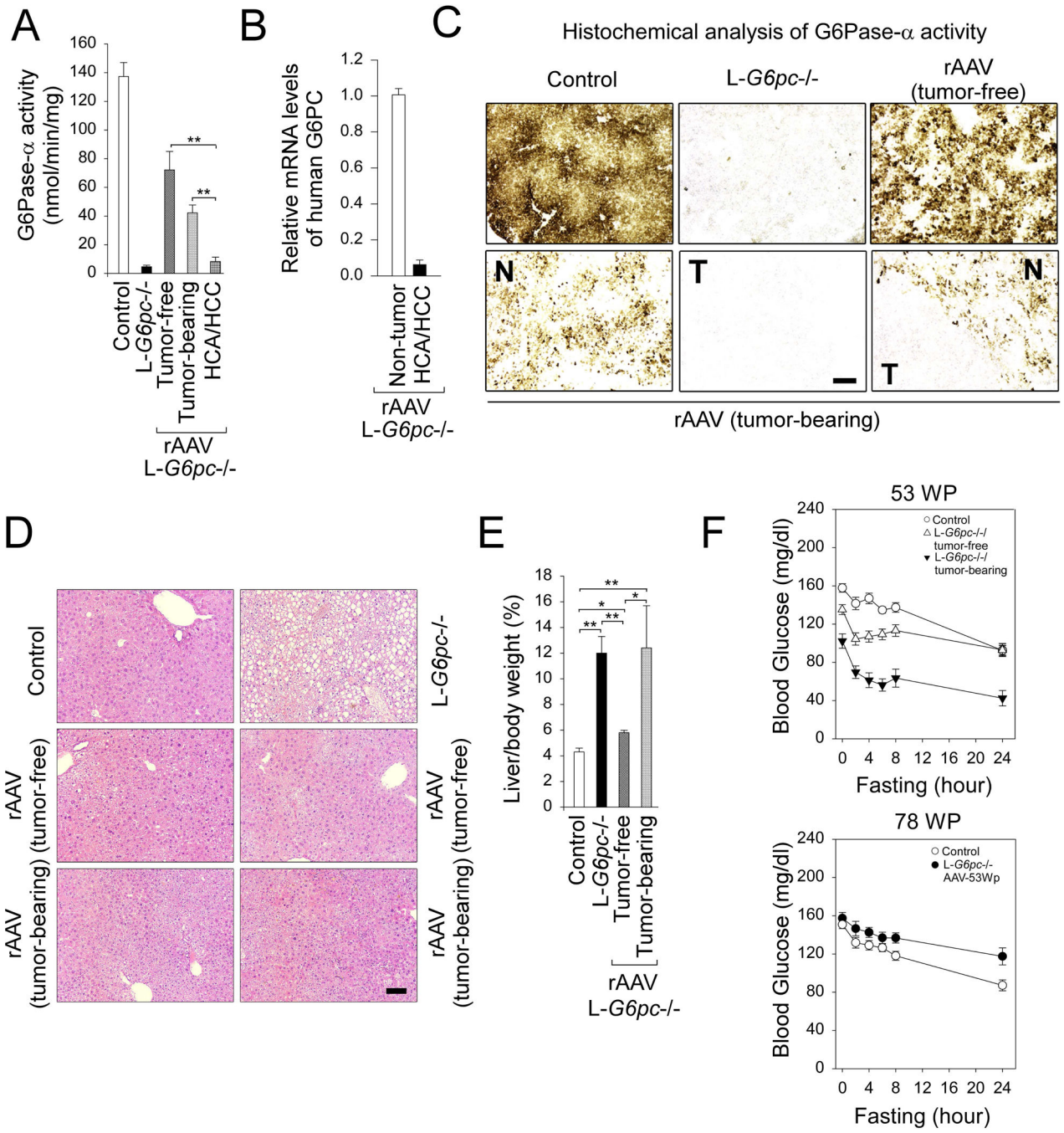

Fig. 3.

rAAV-mediated hepatic G6Pase-α expression prevents de novo HCA/HCC development in L-*G6pc*−/− mice at tumor-developing stage. L-*G6pc*−/− mice were treated with 2×10^{12} vp/kg of rAAV-G6PC at 53 WP and analyzed at 78 WP. (**a**) Hepatic G6Pase-α activity in non-tumor-tissues of control mice (n = 10), untreated L-*G6pc*−/− mice (n = 9), rAAV-treated tumor-free L-*G6pc*−/− mice (n = 8), and rAAV-treated tumor-bearing L-*G6pc*−/− mice (n = 3) as well as in HCA/HCC lesions (n = 4) of rAAV-treated tumor-bearing L-*G6pc*−/− mice. (**b**) Quantification of mRNA for human *G6PC* in HCA/HCC lesions (n = 5) and the adjacent

non-tumor liver tissues (n = 5) of rAAV-treated tumor-bearing L-*G6pc*−/− mice. (**c**) Histochemical analysis of hepatic G6Pase-α activity in liver sections of control, untreated L-*G6pc*−/− mice, rAAV-treated tumor-free L-*G6pc*−/− mice and rAAV-treated tumor-bearing L-*G6pc*−/− mice at 78 WP. T and N denote tumor and nontumor region of rAAV-treated tumor-bearing L-*G6pc*−/− mice, respectively. Scale bar, 200 μm. (**d**) Hematoxylin and eosin (H&E) stained liver sections of control, untreated L-*G6pc*−/− mice, rAAV-treated tumor-free L-*G6pc*−/− mice and rAAV-treated tumor-bearing L-*G6pc*−/− mice at 78 WP. Scale bar, 100 μm. (**e**) Liver weights of control mice (n = 10), untreated L-*G6pc*−/− mice (n = 10), rAAV-treated tumor-free L-*G6pc*−/− mice (n = 8), and rAAV-treated tumor-bearing L-*G6pc*−/− mice (n = 3). (**f**) *Upper:* Fasting glucose tolerance profiles of control (n = 12), tumor-free L-*G6pc*−/− (n = 8) and tumor-bearing L-*G6pc*−/− mice (n = 3) at 53 WP. *Lower:* Fasting glucose tolerance profiles of control (n = 12) mice and rAAV-treated tumor-free and tumor-bearing L-*G6pc*−/− mice (n = 11) at 78 WP. Data represent the mean ± SEM. **P* < 0.05, ***P* < 0.005.

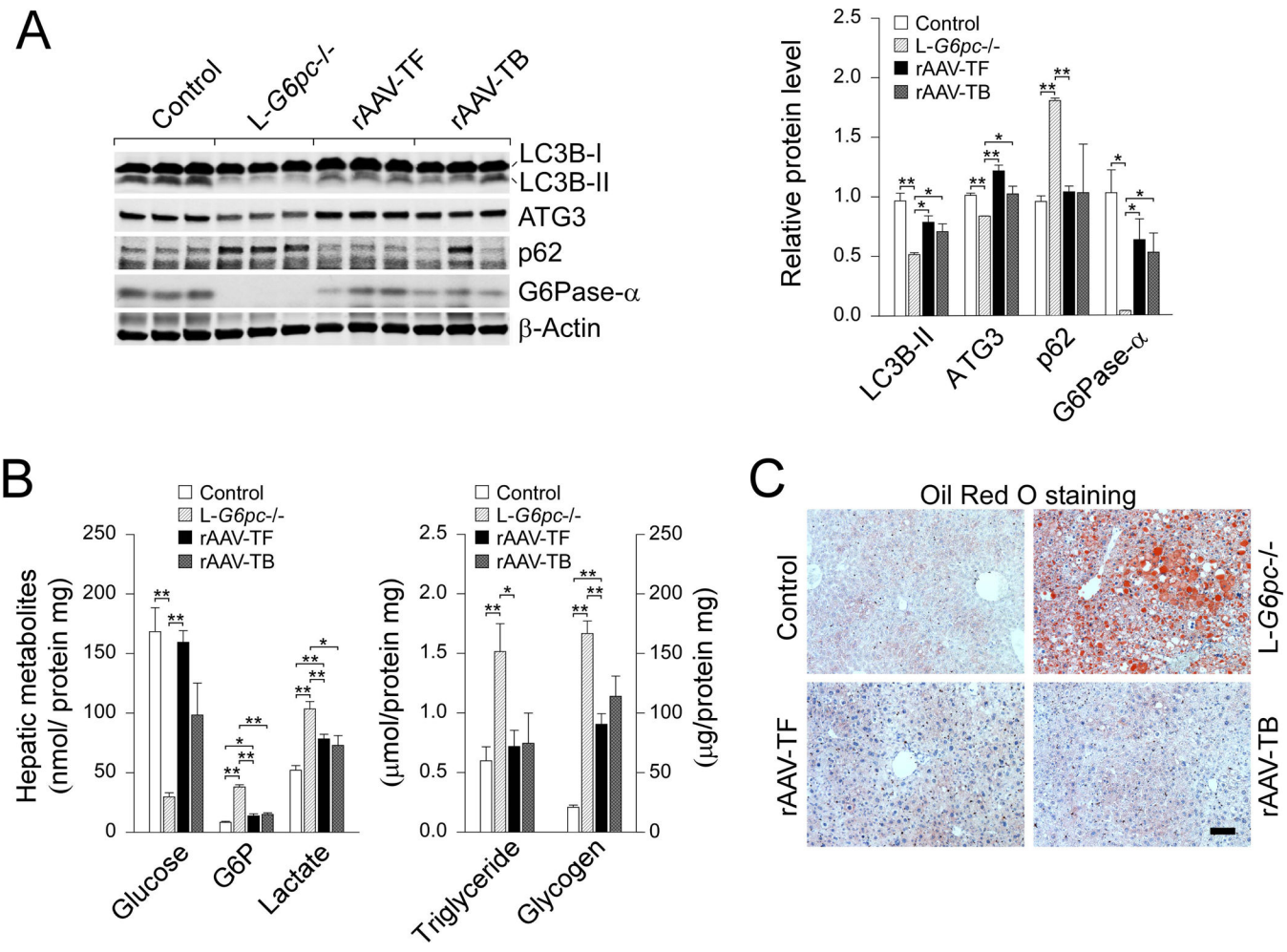

Fig. 4.

Restoration of hepatic G6Pase-α expression corrects metabolic abnormalities and autophagy impairment in L-*G6pc*−/− mice at tumor-developing stage. L-*G6pc*−/− mice were treated with 2×10^{12} vp/kg of rAAV-G6PC at 53 WP and analyzed at 78 WP. (**a**) Western blots of LC3B, ATG3, p62, G6Pase-α and β-actin in the non-tumor liver tissues of control mice and untreated L-*G6pc*−/− mice, rAAV-treated tumor-free L-*G6pc*−/− mice (rAAV-TF), and rAAV-treated tumor-bearing L-*G6pc*−/− mice (rAAV-TB). (**b**) The levels of hepatic metabolites in the non-tumor liver tissues of control mice (n = 9) and untreated L-*G6pc*−/− mice (n = 9), rAAV-treated tumor-free L-*G6pc*−/− mice (rAAV-TF, n = 8) and rAAV-treated tumor-bearing L-*G6pc*−/− mice (rAAV-TB, n = 3) at 78 WP. (**c**) Oil red O staining of indicated liver sections. Scale bar, 100 μm. Data represent the mean ± SEM. **P* < 0.05, ***P* < 0.005.

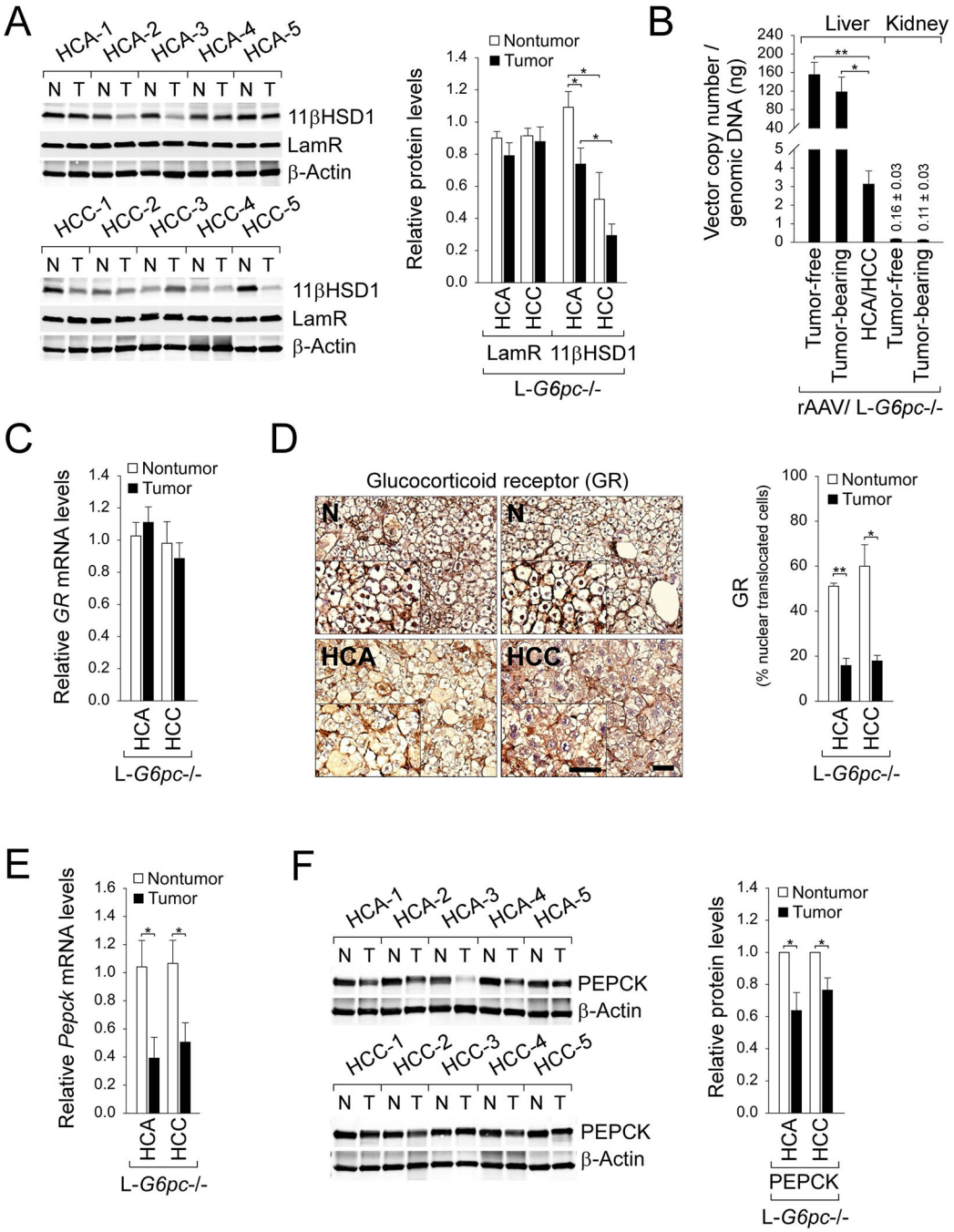

Fig. 5.

Downregulated glucocorticoid signaling in the HCA/HCC lesions developed in L-*G6pc*−/− mice. (**a**) Western blots of 11βHSD1, LamR and β-actin in tumors (T) and the corresponding non-tumor liver tissues (N) of untreated L-*G6pc*−/− mice at 78 WP, and quantification of protein levels by densitometry analysis (nontumor and tumor of HCA or HCC = 5 pairs/each). (**b**) rAAV vector copy numbers per 1 ng of genomic DNA in the non-tumor liver and kidney tissues of rAAV-treated tumor-free L-*G6pc*−/− mice (n = 8), and rAAV-treated tumor-bearing L-*G6pc*−/− mice (n = 3) as well as in HCA/HCC lesions (n = 4) of rAAV-treated

tumor-bearing L-*G6pc*−/− mice. (**c**) Quantification of mRNA for *GR* in HCA (n = 4) and HCC (n = 5) lesions and the corresponding non-tumor liver tissues of untreated L-*G6pc*−/− mice at 78 WP. (**d**) Immunohistochemical analysis of hepatic glucocorticoid receptor (GR) in HCA or HCC lesions in untreated L-*G6pc*−/− mice at 78 WP and quantification of nuclear GR-translocated cells (nontumor and tumor of HCA or HCC = 3 pairs/each). The insets present higher magnification views. Scale bar, 50 μm. (**e**) Quantification of mRNA for *Pepck* in HCA (n = 4) and HCC (n = 5) lesions and the corresponding non-tumor liver tissues of untreated L-*G6pc*−/− mice at 78 WP (**f**) Western blots of PEPCK in tumors (T) and the corresponding non-tumor liver tissues (N) of untreated L-*G6pc*−/− mice at 78 WP, and quantification of protein levels by densitometry analysis (nontumor and tumor of HCA or HCC = 5 pairs/each). Data represent the mean ± SEM. **P* < 0.05, ***P* < 0.005.